

Effect of Injection Depletion in p – n Heterostructures Based on Solid Solutions $(\text{Si}_2)_{1-x-y}(\text{Ge}_2)_x(\text{GaAs})_y$, $(\text{Si}_2)_{1-x}(\text{CdS})_x$, $(\text{InSb})_{1-x}(\text{Sn}_2)_x$, and $\text{CdTe}_{1-x}\text{S}_x$

Sh. N. Usmonov*, A. S. Saidov**, and A. Yu. Leiderman

Starodubtsev Physical-Technical Institute, Uzbekistan Academy of Sciences,
ul. G. Mavlyanova 2, Tashkent, 700084 Uzbekistan

* e-mail: sh_usmonov@rambler.ru

** e-mail: amin@uzsci.net

Received June 9, 2014

Abstract—The current–voltage characteristics of n -Si- p - $(\text{Si}_2)_{1-x-y}(\text{Ge}_2)_x(\text{GaAs})_y$ ($0 \leq x \leq 0.91$, $0 \leq y \leq 0.94$), p -Si- n - $(\text{Si}_2)_{1-x}(\text{CdS})_x$ ($0 \leq x \leq 0.01$), n -GaAs- p - $(\text{InSb})_{1-x}(\text{Sn}_2)_x$ ($0 \leq x \leq 0.05$), and n -CdS- p -CdTe heterostructures have been studied. It has been found that the current–voltage characteristics of these structures contain a portion of sublinear increase in the current with a voltage $V \approx V_0 \exp(Jad)$. The concentrations of deep impurities responsible for the appearance of the sublinear portion of the current–voltage characteristic have been estimated. The experimental results have been explained based on the theory of the injection depletion effect.

DOI: 10.1134/S1063783414120348

1. INTRODUCTION

The injection depletion effect was first theoretically predicted for p – i – n structures operating in the double injection mode [1]. Later, it was experimentally observed in semiconductor structures made of different materials, in particular, zinc-doped silicon [2, 3], gold-doped silicon [4], gallium arsenide [5], silicon–germanium alloy [6], and others. In recent years, this effect was observed in structures fabricated based on different solid solutions, in particular, n -Si- p - $(\text{Si}_2)_{1-x-y}(\text{Ge}_2)_x(\text{GaAs})_y$ [7], p -Si- n - $(\text{Si}_2)_{1-x}(\text{CdS})_x$ [8], p -Si- n - $(\text{GaSb})_{1-x}(\text{Si}_2)_x$ [9], n -GaAs- p - $(\text{InSb})_{1-x}(\text{Sn}_2)_x$ [10], and structures with a CdS–CdTe heterojunction [11].

It is a very specific effect, which immediately follows from its name combining two apparently incompatible notions: injection (of free carriers enriching the structure base) and depletion (i.e., a decrease in the content of free carriers, their removal). This effect is observed only at opposite directions of ambipolar diffusion of excess charge carriers and their ambipolar drift which is controlled by the injection modulation of the charge of deep impurities.

2. CONDITIONS FOR THE INJECTION DEPLETION EFFECT IN p – n STRUCTURES

Injection depletion is observed during double injection in the p – i – n structure at forward current directions; however, its implementation requires that a number of conditions be met. Let us consider the for-

ward-connected p – i – n structure (Fig. 1). According to the terminology proposed by Stafeev, the base (i.e., the i -layer) should not be thin, since the effect occurs exactly in it, but it should not be very long (in this case, as is known, the so-called drift modes of double injection will take place). To observe this effect, the base should be long: $d/L > 1$ (d is the base thickness and L is the diffusion length of excess charge carriers), but it should be not too long, i.e., the ratio d/L should be in the range of 2–7.

Usually, double injection processes in p – n or p – i – n diodes are considered using the basic equation of the problem, which describes the ambipolar behavior of free carriers in the quasi-neutral i -base,

$$D_a \frac{d^2 p}{dx^2} - v_a \frac{dp}{dx} - U = 0, \quad (1)$$

where $D_a = D_n D_p (n + p) / (D_n n + D_p p)$ is the ambipolar diffusion coefficient, $v_a = \mu_a E$ is the ambipolar veloc-

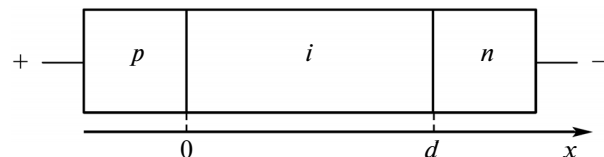


Fig. 1. Schematic representation of the p – i – n structure in the forward direction of the applied voltage; d is the base i -region thickness.

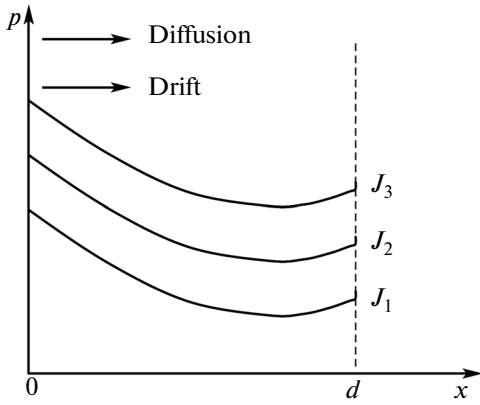


Fig. 2. Distribution of the excess charge carrier concentration along the base i -region of the p - i - n structure in the case where the diffusion and drift of charge carriers are unidirectional at different current densities $J_1 < J_2 < J_3$.

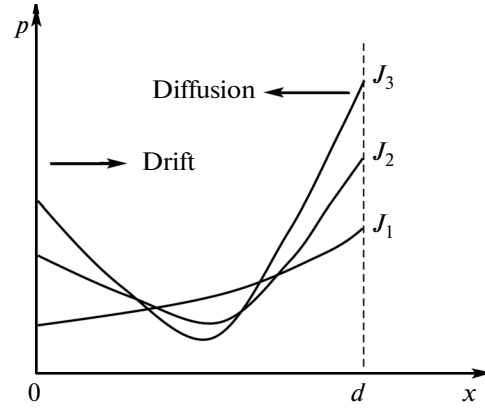


Fig. 3. Distribution of the excess charge carrier concentration along the base i -region of the p - i - n structure in the case where the diffusion and drift of charge carriers are oppositely directed at different current densities $J_1 < J_2 < J_3$.

ity of free carrier drift, $\mu_a = \mu_n \mu_p (n - p) / (\mu_n n + \mu_p p)$ is the ambipolar mobility, $E \approx \frac{J}{q \mu_p (bn + p)}$ is the electric field, J is the current density, and $b = \mu_n / \mu_p$ is the ratio of electron and hole mobilities, respectively.

The notion of ambipolar mobility was used previously by many researchers (see, e.g., [12]).

Usually, in p - n and p - i - n diodes, minority carriers are injected (in the case at hand, holes are chosen for concreteness) and the hole concentration gradient $dp/dx < 0$ is created, since the concentration injected hole density decreases with base depth. Usually, this is exponential decrease such as $\exp\left(-\frac{x}{L_p}\right)$, where $L_p =$

$\sqrt{D_p \tau_p}$ is the hole diffusion length, D_p and τ_p is their diffusion coefficient and lifetime, respectively. Then, the second term in Eq. (1), describing hole drift to the base depth, in fact has the sign “plus,” i.e., ambipolar diffusion described by the first term and ambipolar drift described by the second term have the same sign, and their effects are summed. Physically, this means that free holes arrived at the base are carried away to the second junction under the action of both diffusion and drift. In other words, drift enhances the diffusion effect (Fig. 2). However, for the p - i - n structure, we can mentally imagine the other situation where the free carrier concentration at the i - n junction at which electrons are accumulated at the forward direction under consideration and, due to quasi-neutrality, holes are also accumulated, will become higher than at the p - i junction. This can occur due to different causes to be discussed below. However, if this will occur, the concentration gradient will become positive, $dp/dx > 0$. Then the second term of Eq. (1) will have a negative sign. Physically, this means that diffusion and drift will be oppositely directed (see Fig. 3);

hence, drift and diffusion currents in any voltage range will not enhance as usual, but will suppress each other. Then the free carrier concentration in the base will not increase with current, as is typically the case during injection, but will decrease. From this, the term “injection depletion” arises.

To obtain a mathematical description of this effect, we should return to Eq. (1) and concretize the recombination rate U and ambipolar drift velocity v_a .

Let the recombination rate $U = p/\tau_p$, i.e., has an ordinary form characteristic of the Shockley–Read statistics. As for the ambipolar drift velocity, its general expression is rather complex (see, e.g., [12]),

$$v_a = \left[\frac{\mu_n \mu_p}{\mu_n n + \mu_p p} \right] \left[N_d - \left(\varepsilon \frac{dE}{dx} - p \frac{\partial}{\partial p} \left(\varepsilon \frac{dE}{dx} \right) + M \left(1 - \frac{p}{M} \frac{\partial M}{\partial p} \right) \right) \right] E, \tag{2}$$

where M is the concentration of holes trapped by deep impurities. In this case, one deep level such as the hole trapping center, hence, $M = N_t f_{ip}$, where N_t is the trapping center concentration, $f_{ip} = p/(p + p_{1t})$ is the probability this level population by holes, $p_{1t} = N_v \exp((E_v - E_t)/kT)$ is the Shockley–Read statistical factor for the trapping center level E_t .

As is known, the first term of Eq. (2), proportional to N_d describes the mode of ohmic relaxation of space charge; the second term related to the field variation dE/dx describes the dielectric relaxation of space charge. Finally, the third term is caused exclusively by population modulation of deep impurities. If we restrict the analysis to the case where this term is determining and trapping centers for holes play the

role of such impurity, the expression for the ambipolar drift velocity takes the form

$$v_a = \frac{I}{q} \frac{\mu_n \mu_p N_t}{(\mu_n + \mu_p)^2 (p_{it}^*)^2}, \quad (3)$$

where $p_{it}^* = p_{it} + \frac{\mu_n}{\mu_n + \mu_p} N_t$.

Under conditions of the dominant effect of modulation of deep trapping centers whose trapping factor

$\gamma = \frac{N_t}{p_{it}} \gg 1$ and at $p < p_{it}^*$, the expressions for the

ambipolar drift velocity and diffusion become simpler: $v_a \approx aJD_a$ and $D_a \approx D_p$. In this case, Eq. (1) takes the relatively simple form

$$\frac{d^2 p}{dx^2} - aJ \frac{dp}{dx} - \frac{p}{\tau} = 0, \quad (4)$$

where

$$a = \frac{1}{2qD_p N_t} \quad (5)$$

is the parameter depending only on the total concentration N_t of deep trapping centers and on the diffusion coefficient D_p of majority carriers (i.e., on their mobility, $D_p = kT\mu_p/q$).

At sufficiently high currents when $Jad > 2$, the approximate solution to Eq. (4) has the form [1, 12]

$$p \sim \exp(-aJx), \quad (6)$$

i.e., the concentration of injected carriers decreases as the current increases (Fig. 3). At base edges, at the boundaries with $p-i$ and $i-n$ junctions, this value increases as usual, i.e., the boundary concentrations $p(0)$ and $p(d)$ increase with current, but decreases at the center. Accordingly, the voltage drop at the base is [1, 12]

$$V \approx V_0 \exp(Jad), \quad (7)$$

where

$$V_0 = \frac{kT}{q} 2b \left[\frac{qV_p^* (1 + \gamma) N_t^2}{(b\gamma + b + 1)n_n J} \right]^{1/2}, \quad (8)$$

and V_p^* is effective velocity of hole leakage through the $i-n$ junction.

Thus, due to the very simple shape of the current-voltage characteristic and the simple dependence of the parameter a on the deep impurity concentration N_t , this effect can be easily observed and validated experimentally.

Let us dwell on the possibility of creating conditions for implementing this effect. The main thing in these conditions is the sign change in the free carrier concentration gradient. To implement this, the $i-n$

junction should be "good," i.e., it should supply many electrons, whereas the $p-i$ junction should be "bad," i.e., it should inject a small number of holes. This situation can be implemented originally technologically, but also can arise during device operation. As is known, in the case of perfect junctions, $p(0) \sim J$ and $p(d) \sim J$ (see, e.g., [12]); for imperfect junctions, these dependences get weaker, $p(0) \sim \sqrt{J}$ and $p(d) \sim \sqrt{J}$. If the junction becomes imperfect ($p(0) \sim \sqrt{J}$) while the $i-n$ junction remains perfect ($p(d) \sim J$), the carrier concentration at the $i-n$ junction can become higher than that at the $p-i$ junction; accordingly, the gradient dp/dx sign becomes positive, i.e., conditions for the injection depletion effect are satisfied.

3. SAMPLE PREPARATION AND EXPERIMENTAL TECHNIQUE

For experimental investigations of the injection depletion effect, $p-n$ heterostructures were fabricated based on the following solid solutions: $n\text{-Si-}p\text{-(Si}_2\text{)}_{1-x-y}\text{(Ge}_2\text{)}_x\text{(GaAs)}_y$ ($0 \leq x \leq 0.91$, $0 \leq y \leq 0.94$), $p\text{-Si-}n\text{-(Si}_2\text{)}_{1-x}\text{(CdS)}_x$ ($0 \leq x \leq 0.01$), $n\text{-GaAs-}p\text{-(InSb)}_{1-x}\text{(Sn}_2\text{)}_x$ ($0 \leq x \leq 0.05$), and $n\text{-CdS-}p\text{-CdTe}$.

The $n\text{-Si-}p\text{-(Si}_2\text{)}_{1-x-y}\text{(Ge}_2\text{)}_x\text{(GaAs)}_y$ heterostructures were fabricated by growing a $p\text{-(Si}_2\text{)}_{1-x-y}\text{(Ge}_2\text{)}_x\text{(GaAs)}_y$ ($0 \leq x \leq 0.91$, $0 \leq y \leq 0.94$) solid solution on $n\text{-Si}$ substrates with resistivity $0.5 \Omega \text{ cm}$ and $\sim 400 \mu\text{m}$ thick by vapor-phase epitaxy from a limited volume of Pb-Si-Ge-GaAs solution-melt in a hydrogen atmosphere purified by palladium. The crystallization onset temperature of the epitaxial layer was 850°C , the solution-melt cooling rate was equal to 1°C/min , the solution-melt thickness (the gap between horizontally arranged substrates) was $1\text{--}1.5 \text{ mm}$. The grown layer thickness was $\sim 25 \mu\text{m}$, the resistivity was $\sim 0.5 \Omega \text{ cm}$, and the conductivity was p -type. Current-collecting contacts made by vacuum deposition ($\sim 10^{-5}$ Torr) of silver were continuous from the backside and quadrangular (with an area of $\sim 12 \text{ mm}^2$) from the epitaxial layer side. Basic materials for the heterostructure were $p\text{-(Si}_2\text{)}_{1-x-y}\text{(Ge}_2\text{)}_x\text{(GaAs)}_y$ epitaxial films.

The current-voltage characteristic of the heterostructure, shown in Fig. 4 was measured in forward and reverse directions in a wide range of current and voltage variations. The study was performed in the dark at room temperature.

The $p\text{-Si-}n\text{-(Si}_2\text{)}_{1-x}\text{(CdS)}_x$ heterostructures were fabricated by growing a $n\text{-(Si}_2\text{)}_{1-x}\text{(CdS)}_x$ ($0 \leq x \leq 0.01$) solid solution by vapor-phase epitaxy from a limited volume of Sn-Si-CdS solution-melt on $p\text{-Si}$ substrates with a resistivity of $10 \Omega \text{ cm}$ and $\sim 350 \mu\text{m}$ thick in a hydrogen atmosphere purified by palladium. The crystallization onset temperature of the epitaxial layer was 1150°C , the solution-melt cooling rate was 1°C/min , and the solution-melt thickness was 1 mm .

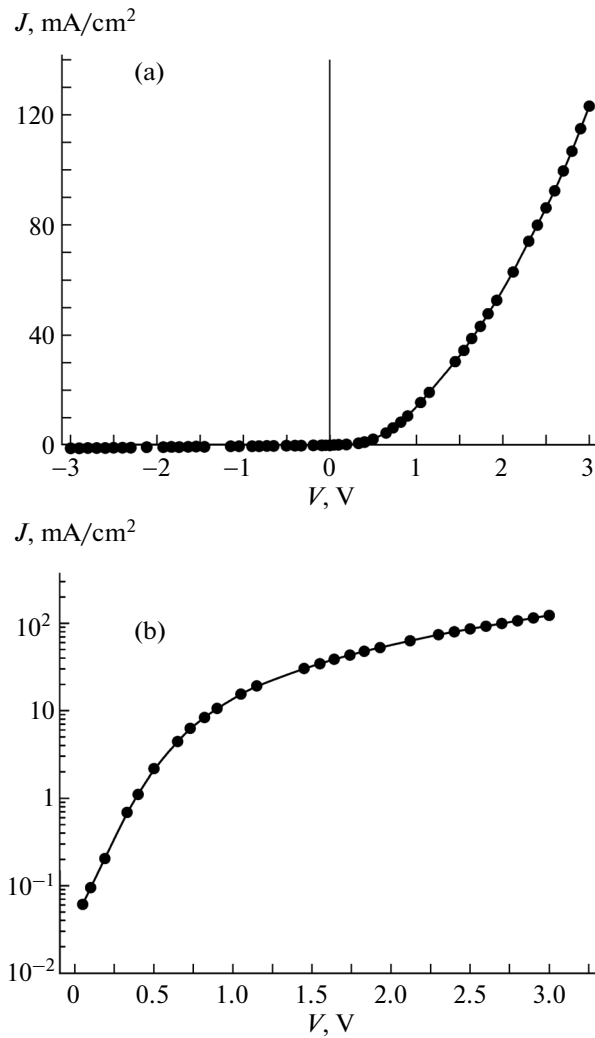


Fig. 4. (a) Dark current–voltage characteristic of the n -Si- p - $(\text{Si}_2)_{1-x-y}(\text{Ge}_2)_x(\text{GaAs})_y$ ($0 \leq x \leq 0.91$, $0 \leq y \leq 0.94$) heterostructure and (b) its forward portion in semilogarithmic coordinates at room temperature.

The grown layer thickness was $\sim 25 \mu\text{m}$, the resistivity was $\sim 0.016 \Omega \text{ cm}$, and the conductivity was n -type. Current-collecting contacts made by vacuum deposition ($\sim 10^{-5}$ Torr) of silver were continuous from the backside and quadrangular (with an area of $\sim 10 \text{ mm}^2$) from the epitaxial layer side. Basic materials for the heterostructure were n - $(\text{Si}_2)_{1-x}(\text{CdS})_x$ epitaxial films.

The current–voltage characteristic of the heterostructure, shown in Fig. 5, was measured in the forward and reverse directions in a wide range of current and voltage variations. The study was performed in the dark at room temperature.

The n -GaAs- p - $(\text{InSb})_{1-x}(\text{Sn}_2)_x$ heterostructures were fabricated by growing a p - $(\text{InSb})_{1-x}(\text{Sn}_2)_x$ ($0 \leq x \leq 0.05$) solid solution by vapor-phase epitaxy from a limited volume of In–InSb solution–melt on n -GaAs substrates with a free carrier concentration of $(4\text{--}7) \times$

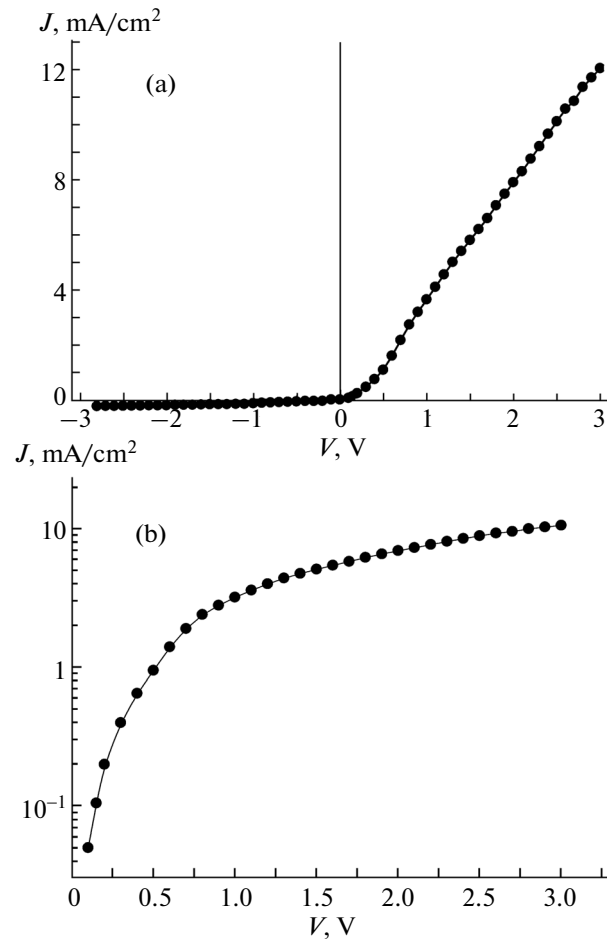


Fig. 5. (a) Dark current–voltage characteristic of the p -Si- n - $(\text{Si}_2)_{1-x}(\text{CdS})_x$ ($0 \leq x \leq 0.01$) heterostructure and (b) its forward portion in semilogarithmic coordinates at room temperature.

10^{17} cm^{-3} and (100) crystallographic orientation in a hydrogen atmosphere purified by palladium. The crystallization onset temperature of the epitaxial layer was 325°C , the solution–melt cooling rate was $1^\circ\text{C}/\text{min}$, and the solution–melt thickness was 1 mm . The grown layer thickness was $\sim 12 \mu\text{m}$, and the conductivity was p -type.

Current-collecting contacts made by fusing indium droplets into the structure. Basic materials for the heterostructure were p - $(\text{InSb})_{1-x}(\text{Sn}_2)_x$ epitaxial films.

The current–voltage characteristic of the heterostructure, shown in Fig. 6, was measured in the forward direction in a wide range of current and voltage variations. The study was performed in the dark at room temperature.

The n -CdS- p -CdTe heterojunctions were fabricated by the technology described in [13]. Large-block p -CdTe films with a resistivity of $\sim 10^2\text{--}10^3 \Omega \text{ cm}$ and $\sim 70 \mu\text{m}$ thick were grown on molybdenum substrates by sublimation in a hydrogen flow. The films consist of

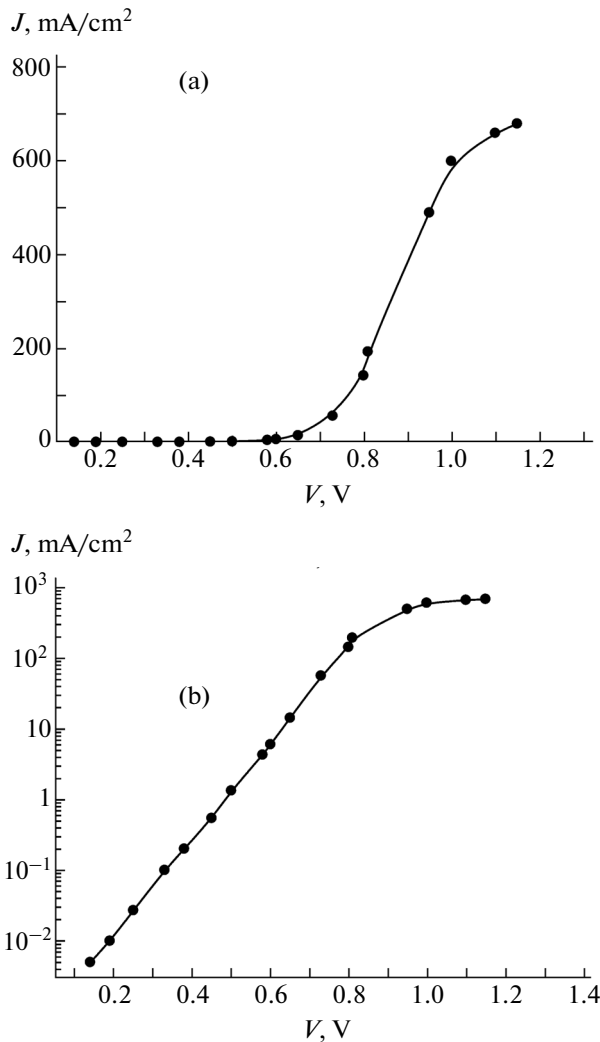


Fig. 6. (a) Dark current–voltage characteristic of the n -GaAs– p –(InSb) $_{1-x}$ (Sn $_2$) $_x$ ($0 \leq x \leq 0.05$) heterostructure and (b) its forward portion in semilogarithmic coordinates at room temperature.

microcrystal blocks with a columnar structure of grains oriented in the growth direction and misoriented in azimuth. Grain sizes are from 100 to 150 μm . A n -CdS was deposited on the p -CdTe film surface in a quasi-closed volume in a vacuum of 10^{-5} Torr by thermal evaporation. The source temperature was maintained at 910°C , the substrate temperature was 180°C . The top current-collecting contact (from the n -CdS layer side) was fabricated by indium sputtering in vacuum ($\sim 10^{-5}$ Torr) in the Π -shaped configuration. Molybdenum was used as a rear contact.

The current–voltage characteristic of the heterostructure, shown in Fig. 7, was measured in the forward and reverse directions in a wide range of current and voltage variations. The study was performed in the dark at room temperature.

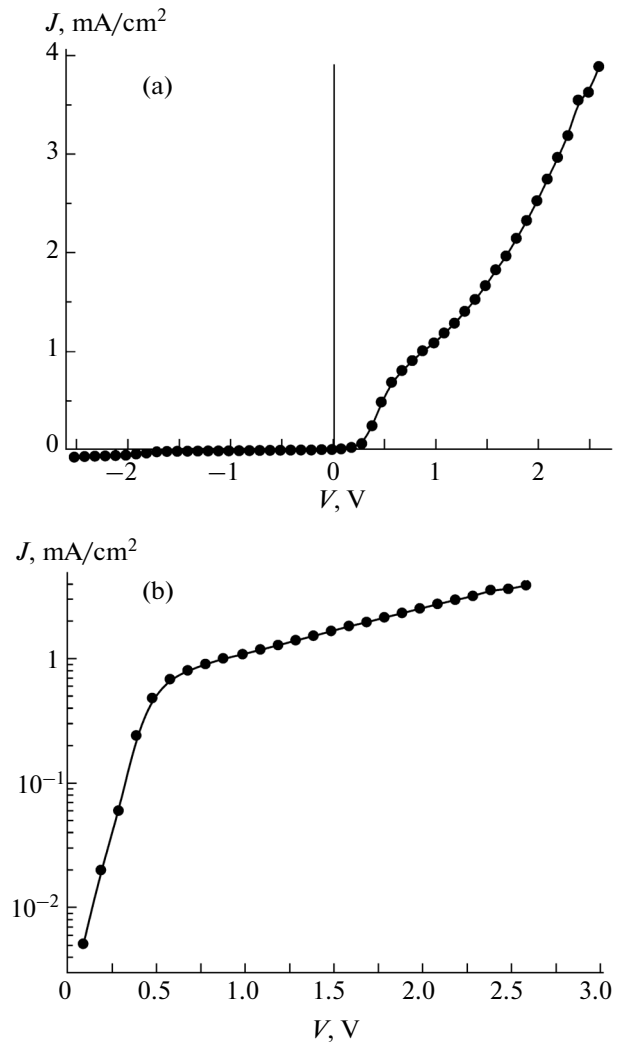


Fig. 7. (a) Dark current–voltage characteristic of the n -CdS– p -CdTe heterostructure and (b) its forward portion in semilogarithmic coordinates.

4. EXPERIMENTAL RESULTS AND DISCUSSION

An analysis of forward portions of current–voltage characteristics of the studied heterostructures (Figs. 4b, 5b, 6b, 7b) shows that their initial portion ($V < 0.4$ V for n -Si– p –(Si $_2$) $_{1-x-y}$ (Ge $_2$) $_x$ (GaAs) $_y$, $V < 0.2$ V for p -Si– n –(Si $_2$) $_{1-x}$ (CdS) $_x$, $V < 0.8$ V for n -GaAs– p –(InSb) $_{1-x}$ (Sn $_2$) $_x$, $V < 0.4$ V for n -CdS– p -CdTe heterostructures) is well approximated by the exponential dependence [14]

$$I = I_0 \exp\left(\frac{qV}{ckT}\right), \quad (9)$$

where q is the elementary charge, V is the electric voltage applied to the structure, k is the Boltzmann constant, and T is the absolute temperature. Dependence (9) is characteristic of the p – n diode with modulated

Exponents c in formula (9) and electrical resistivities of the high-resistance base of the structures under study

Parameter	$n\text{-Si-}p\text{-(Si}_2\text{)}_{1-x-y}\text{(Ge}_2\text{)}_x\text{(GaAs)}_y$	$p\text{-Si-}n\text{-(Si}_2\text{)}_{1-x}\text{(CdS)}_x$	$n\text{-GaAs-}p\text{-(InSb)}_{1-x}\text{(Sn)}_x$	$n\text{-CdS-}p\text{-CdTe}$
c	4.5	2.8	2.5	3.2
$\rho, \Omega \text{ cm}$	3.7×10^9	6.7×10^7	17	8.9×10^7

resistivity of the high-resistance “long” ($d/L_n > 1$) base. The electronic processes caused by charge modulation when current passes through the structure are mainly controlled by the intermediate high-resistance layer between the substrate and epitaxial layer and solid solutions. The values of the exponent c , calculated from the initial portion of the forward portion of current–voltage characteristic (9) for the different structures are listed in the table.

The pre-exponential factor I_0 in dependence (9) is described by the expression [14]

$$I_0 = \frac{kT}{q} \frac{Sbc \cosh(d/L_n)}{2(b+1)L_n \rho \tan(d/2L_n)}, \quad (10)$$

where S is the sample area and ρ is the resistivity. Using relation (10), the base resistivities of the studied structures were calculated, which are also given in the table. We can see that a high-resistance layer of corresponding solid solutions is formed in the base region of the structures between the substrate and low-resistance epitaxial film.

In Figs. 4b, 5b, 6b, and 7b showing the semilog forward portions of current–voltage characteristics, we can see that an extended sublinear region appears after the exponential dependence on all current–voltage characteristics, where the current slightly varies with increasing applied voltage ($V > 2$ V for $n\text{-Si-}p\text{-(Si}_2\text{)}_{1-x-y}\text{(Ge}_2\text{)}_x\text{(GaAs)}_y$, $V > 2.5$ V for $p\text{-Si-}n\text{-(Si}_2\text{)}_{1-x}\text{(CdS)}_x$, $V > 1$ V for $n\text{-GaAs-}p\text{-(InSb)}_{1-x}\text{(Sn)}_x$ and $n\text{-CdS-}p\text{-CdTe}$ heterostructures). This region can be well described within the above-stated theory, i.e., the injection depletion effect (7).

Using expression (7), we can determine the parameter a immediately from the experimental current–voltage characteristic,

$$a = \frac{\ln(V_2/V_1)}{(J_2 - J_1)d}, \quad (11)$$

where J_1 and J_2 are the current densities at voltages V_1 and V_2 at neighboring points of the sublinear region of the current–voltage characteristic.

Since the carrier diffusion coefficient depends only on temperature and majority carrier mobility, having determined the parameter by relation (5), we can find the product of the majority carrier mobility and deep impurity concentration, μN_i .

In the $n\text{-CdS-}p\text{-CdTe}$ heterostructure, a high-resistance intermediate layer with a resistivity of $8.9 \times$

$10^7 \Omega \text{ cm}$ (see table) is formed of a $\text{CdTe}_{1-x}\text{S}_x$ solid solution [13, 15–17] between $n\text{-CdS}$ and $p\text{-CdTe}$ layers and it mainly controls electronic processes in the structure as a whole, including the current transport mechanism. The parameter a of the sublinear region of the current–voltage characteristic of the $n\text{-CdS-}p\text{-CdTe}$ heterostructure (Fig. 7b) was $a \approx 1.6 \times 10^6 \text{ cm/A}$, and the deep center concentration was $N_i \approx 1.3 \times 10^{13} \text{ cm}^{-3}$. In the $\text{CdTe}_{1-x}\text{S}_x$ solid solution, deep levels are formed by unintentional impurities Cu, Ag, Au whose ionization energies are $E_i \approx 0.3\text{--}0.4 \text{ eV}$, and by a doubly charged cadmium vacancy (V_{Cd}^{2-}) with an ionization energy $E_i \approx 0.6 \text{ eV}$ [18]. As was shown in [11], the study of the sublinear region of the current–voltage characteristic of such structures made it possible to determine that the product $\mu_n N_i$ increases by two orders of magnitude with increasing temperature in the range of 293–430 K. Taking into account that a large number of defect complexes are inherent to II–VI materials, in particular, “impurity–vacancy” complexes [19], it can be assumed that heating releases new vacancies which are responsible for the observed effect.

The parameter a determined based on the experimental data of Fig. 5b for the $p\text{-Si-}n\text{-(Si}_2\text{)}_{1-x}\text{(CdS)}_x$ ($0 \leq x \leq 0.01$) heterostructure was $a \approx 4.4 \times 10^4 \text{ cm/A}$, then $\mu_n N_i \approx 2.74 \times 10^{15} \text{ V}^{-1} \text{ cm}^{-1} \text{ s}^{-1}$. The majority carrier mobility (electrons of solid solution $n\text{-(Si}_2\text{)}_{1-x}\text{(CdS)}_x$), determined by the Hall method, was $\mu_n \approx 300 \text{ cm}^2/\text{Vs}$; hence, the concentration of deep impurities causing the injection depletion effect is $N_i \approx 9.13 \times 10^{12} \text{ cm}^{-3}$. In [20], diffraction patterns of $\text{Si}_{1-x}\text{Sn}_x$ solid solution grown from a tin solution–melt were studied. It was found that tin can not only substitute site silicon atoms, but also are segregated at sites between blocks of silicon atoms, at interphase boundaries, and can appear at interstices. These facts suggest that tin will always behave as a neutral substitution atom in the $(\text{Si}_2)_{1-x}\text{(CdS)}_x$ solid solution. It is possible that, being at interphase boundaries, it will behave as an ordinary deep impurity and will be responsible for the observed sublinear current–voltage characteristic.

The parameter a determined by formula (11) based on the experimental data of Fig. 4b for the $n\text{-Si-}p\text{-(Si}_2\text{)}_{1-x-y}\text{(Ge}_2\text{)}_x\text{(GaAs)}_y$ ($0 \leq x \leq 0.91$, $0 \leq y \leq 0.94$) heterostructure was $a \approx 3.2 \times 10^3 \text{ cm/A}$; then, according to relation (5), we obtain $\mu_p N_i \approx 3.77 \times 10^{16} \text{ V}^{-1} \text{ cm}^{-1} \text{ s}^{-1}$. The majority carrier mobility (holes

of the p -(Si_2) $_{1-x-y}$ (Ge_2) $_x$ (GaAs) $_y$ solid solution) determined by the Hall method was $\mu_p \approx 55 \text{ cm}^2/\text{V s}$. Knowing μ_p , we can find the concentration of impurities having deep energy levels, responsible for the injection depletion effect in the studied structure. At room temperature, it was $N_i \approx 6.85 \times 10^{14} \text{ cm}^{-3}$. Since this structure was fabricated based on a solid solution grown from a lead solution–melt, we can assume that lead, similarly to tin in the (Si_2) $_{1-x}$ (CdS) $_x$ solid solution is responsible for the formation of these impurities.

The parameter a for the n - GaAs – p -(InSb) $_{1-x}$ (Sn_2) $_x$ ($0 \leq x \leq 0.05$) heterostructure (Fig. 6b) was $a \approx 1.27 \times 10^3 \text{ cm/A}$. The product of the mobility of majority carriers (holes of p -(InSb) $_{1-x}$ (Sn_2) $_x$ solid solution) and the deep impurity concentration is $\mu_p N_i \approx 9.57 \times 10^{16} \text{ V cm}^{-1} \text{ s}^{-1}$. Taking into account the high hole mobility in InSb ($\mu_p \approx 750 \text{ cm}^2/(\text{V s})$), we can estimate the approximate concentration $N_i \approx 10^{14} \text{ cm}^{-3}$. It is possible that tin interstitials are also responsible for the appearance of these impurities, as in the case of (Si_2) $_{1-x}$ (CdS) $_x$ solid solution.

5. CONCLUSIONS

The performed investigations allowed us to conclude that the injection depletion effect is observed in a significant voltage range for all heterostructures studied, despite the considerable differences in the initial materials, conductivity types, and fabrication technologies. To understand the nature of deep impurities responsible for the observed effect, further studies are required. In particular, since the strong influence of different external exposures (temperature, photoexcitation, magnetic field, and others) on this effect is known [12], such studies will certainly facilitate the understanding of the nature of these impurities.

ACKNOWLEDGMENTS

This study was supported by the Committee for Coordination of Science and Technology Development of the Republic of Uzbekistan (basic research grant no. F2-FA-0-43917).

REFERENCES

1. A. Yu. Leiderman and P. M. Karageorgiy-Alkalaev, *Solid State Commun.* **27**, 339 (1976).
2. P. M. Karageorgiy-Alkalaev, I. Z. Karimova, P. I. Knigin, and A. Yu. Leiderman, *Phys. Status Solidi A* **34** (1), 391 (1976).
3. A. A. Abakumov, P. M. Karageorgiy-Alkalaev, I. E. Karimova, P. I. Knigin, and A. Yu. Leiderman, *Sov. Phys. Semicond.* **10** (3), 200 (1976).
4. M. E. Gilenko, P. M. Karageorgiy-Alkalaev, and A. Yu. Leiderman, *Phys. Status Solidi A* **78** 1, K165 (1981).
5. V. V. Morozkin, *Dokl. Akad. Nauk UzSSR*, No. 4, 40 (1976).
6. A. S. Saidov, A. Yu. Leiderman, B. Sapaev, S. Zh. Karazhanov, and D. V. Saparov, *Semiconductors* **30** (6), 550 (1996).
7. A. S. Saidov, A. Yu. Leiderman, Sh. N. Usmonov, and K. T. Kholikov, *Dokl. Akad. Nauk Resp. Uzb.*, No. 5, 23 (2008).
8. A. S. Saidov, A. Yu. Leyderman, Sh. N. Usmonov, and K. T. Kholikov, *Semiconductors* **43** (4), 416 (2009).
9. Sh. N. Usmonov, A. S. Saidov, A. Yu. Leyderman, D. Saparov, and K. T. Kholikov, *Semiconductors* **43** (8), 1092 (2009).
10. A. S. Saidov, M. S. Saidov, Sh. N. Usmonov, and U. P. Asatova, *Semiconductors* **44** (7), 938 (2010).
11. Sh. N. Usmonov, Sh. A. Mirsagatov, and A. Yu. Leyderman, *Semiconductors* **44** (3), 313 (2010).
12. E. I. Adirovich, P. M. Karageorgiy-Alkalaev, and A. Yu. Leiderman, *Double Injection Currents in Semiconductors* (Sovetskoe Radio, Moscow, 1978) [in Russian].
13. Zh. Zhanabergenov and Sh. A. Mirsagatov, in *Proceedings of Conference "Fundamental and Applied Problems of Physics," Tashkent, Uzbekistan, 2003*.
14. V. I. Stafeyev, *Sov. Phys. Tech. Phys.* **3** (9), 1502 (1958).
15. M. K. Herndon, A. Gupta, V. I. Kaydanov, and R. T. Collins, *J. Appl. Phys. Lett.* **75** (22), 3503 (1999).
16. K. Ohata, J. Sarate, and T. Tanaka, *Jpn. J. Appl. Phys.* **12**, 1641 (1973).
17. S. A. Muzafarova and Sh. A. Mirsagatov, *Ukr. J. Phys.* **51**, 1125 (2006).
18. K. Zanio, in *Semiconductors and Semimetals*, Ed. by R. K. Willardson (Academic, London, 1978), Vol. 4.
19. *Physics of II–VI Compounds*, Ed. by A. N. Georgibiani and M. K. Sheikman (Nauka, Moscow, 1986) [in Russian].
20. A. S. Saidov, Sh. N. Usmonov, M. U. Kalanov, A. N. Kurmantayev, and A. N. Bahtybayev, *Phys. Solid State* **55** (1), 36 (2013).

Translated by A. Kazantsev